ANALELE UNIVERSITĂȚII
"EFTIMIE MURGU" REȘIȚA
ANUL XXII, NR. 1, 2015, ISSN 1453 - 7397

Mohammad Etemadi, Fakhri Etemadi, Tayeb Pourreza

Vibration and Buckling Analysis of Moderately Thick Plates using Natural Element Method

Using natural element method (NEM), the buckling and the free vibration behaviors of moderate thick plates is studied here. The basis of NEM is natural neighbors and Voronoi cells concepts. The shape functions of nodes located in the domain is equal to the proportion of common natural neighbors area divided by area that related by each Voronoi cells. First step in analyzing the moderate thick plates is identification boundaries. This is done by nodes scattering on problem domain. Mindlin/Reissner theory is used to express the equations of moderate thick plate. First and second order shape functions obtained from natural element method are used to discretize differential equations. Using numerical integration on whole discrete equations of domain, stiffness, geometry and mass matrices of plate are obtained. Buckling loads and vibration modes are expressed by substituting these matrices in plate equations of motions. Arbitrary shapes of plate are selected for solution. Comparing the results of the current approach with those obtained by other numerical analytical methods, it is shown that natural element method can solve problems with complex areas accurately.

Keywords: *natural vibration, buckling, natural elements, Voronoy cells*

1. Introduction

For many years Finite Element Method was used for modulation of different fields of engineering. However in recent years, various meshless methods were developed to avoid mesh related difficulty such as large deformations phenomena that was occurred in FEM.[1]. In FE Methods, the connectivity of finite element equations in meshes should be determined. However, the user is not needed to determine the equations between nodes in meshless or Mesh Free Methods (MFM). So, compared with FEM, MFM can be applied easier by the user. (NEM) which is a mesh free method was presented by (Braun) and (Sambridg) [2]. (Sukumar), (Moran) and (Belystchko) used this method to analyze two-dimensional plate with

cracks [3]. NEM has been used in various mechanical engineering fields including elastostatics and elastodynamics problems for different purposes such as crack propagation and large deformations problems. Cho and Lee [4] used the NEM to calculate frequency and vibration modes of isotropic membrane plate. They applied some simplifying assumptions, such as constant bending in each region of Voronoi cells. Based on this method, equation of motion of plate was found. Moreover this method was used to analyse coupled radiative and conductive heat transfer [5].chen et al used natural neighbour interpolation method for analysis of PZT structures[6].In this paper, the NEM is applied to analyze the buckling and vibration be3haviors of thick plate with different boundary conditions. NEM Shape functions are determined based on the number of nodes that scattered in the field of problem. Governing equations showing behavior of plate are discretized based on the shape function of each node. Geometric, stiffness and mass matrices are obtained from the numerical integration on the whole problem domain and then critical buckling loads and vibration modes of plate are derived. To achieve this purpose, different techniques are used to consider plates behaviors such as analytical methods like Navier (Navier) (Reddy and Phan, 1985)[7]and Levy (Levy) (Liew et al., 1996; Zenkour, 2001)[8 and 9]. These exact methods have been used in solving the equations of rectangular plates by applying specific boundary conditions. Different geometries and boundary conditions are applied on many practical and engineering problems. In addition to exact methods, some researchers have used numerical methods to solve these kinds of problems. Kirchhoff and Mindlin theories are theoretical and numerical methods that are used to analyze the behavior of customary plates used in industry. In Kirchhoff theory, shear strain is considered zero. This assumption makes the equilibrium equation more simplified and applicable for thin plates. As shear strain is a prominent parameter in thick plate analyses, this simplification could not be appropriate in thick plate analyses. Using Mindlin theory, shear strain is considered here and reduction integration method was applied for thin plate analysis. This theory can describe plate behavior, but researchers prefer to use numerical method such as Finite element, MFM to solve plates' equation of motions. Based on their ability to model different boundary conditions, different numerical methods have been considered. The outline of this paper is as follows: in Section 2 nodal connectivity for natural neighbors based on the delaunay triangles and the algorithm of interpolation shape functions construction is presented. In Section 3, the governing equations of plate based on FSDT and the matricial procedure to obtain the equilibrium equation system is presented. In Section 4, 5, brief description about algorithm of program is expressed and the NEM numerical efficiency is shown. In this section Numerical examples are presented and discussed to depict the accuracy and effectiveness of the NEM method.

2. Natural element method interpolation

The interpolation based on NE Method is constructed on the basis of the Voronoi cell concept. A cloud of separated nodes $N=\{n_1,n_2,...,n_N\}$ has been tessellated on the region of problem R^2.first Voronoi diagram of node n_1 calculate based on the closer region T_1 around of node n_1 rather than others nodes.

$$T_i=\{\, x\in R^2 \,|\, d(x,x_i)<d(x,x_j)\,\forall J\neq I\,\} \tag{1}$$

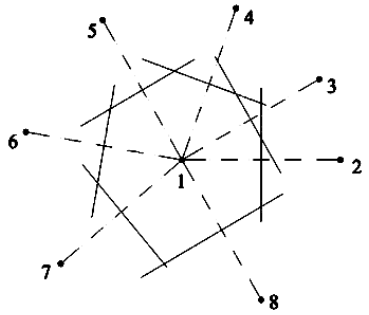

Figure 1. Voroni diagram of node 1

Where Euclidean metric of $d(x_I,x_J)$ is the distance between xi and xJ. The Delaunay triangulation is the topological dual of the Voronoi diagram.Delaunay tessellations based on connecting the nodes whose Voronoi cells have common boundaries are obtained. [10]. In figure (2) first Voronoi cells Delaunay triangles have been shown by dashed and bold lines, respectively.

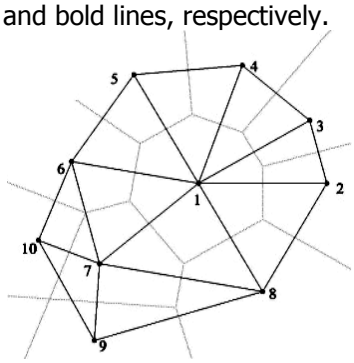

Figure 2. Voroni cell and Delaunay triangle tessellation

If another point like Y is added to pervious region, second order of Voroni would be constraucted. In figure (3), second Voronoi cell of point Y that isadded to previous nodes would be obtained by region that has been confined form perpendicular bisector of the connection line between point Y to around vicinities nodes (node 10, 8,7,6,1 or polygon wise of abcde). Shape function of node I related to point Y is obtained from overlapped area of first Voroni cell of node I and second Voronoi cell of point Y on whole area of second Voronoi cell

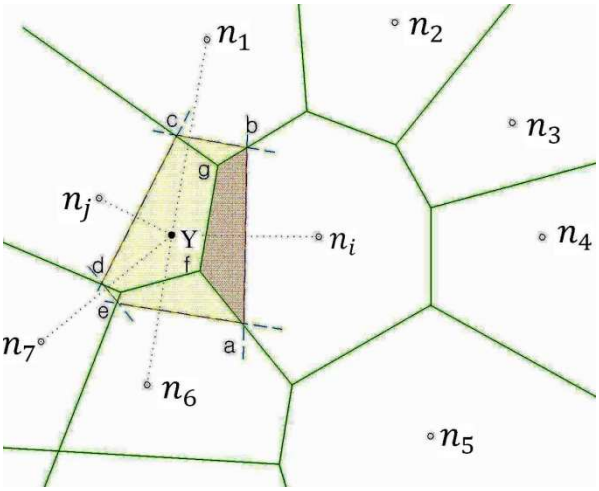

Figure 3. second voroni cell for point Y

$$\varphi_{I(x)} = \frac{A_{I(x)}}{A_{(x)}} \quad , \quad I = 1,2,..., N \tag{2}$$

$$A_{(x)} = \sum_{I=1}^{n} A_{I(x)} \tag{3}$$

For example, the shape function of node i related to point Y is defined as:

$$\varphi_1(x) = \frac{A_{abgf}}{A_{abcde}} \tag{4}$$

Higher-order derivatives of shape functions in two directions of x and y axis are obtained from:

$$\varphi_{I,\alpha}(x) = \frac{A_{I,\alpha}(x) - \varphi_I(x) A_{,\alpha}(x)}{A(x)} \quad \alpha = 1,2 \tag{5}$$

3. Mindlin plate element formulations

3.1. Laminated plate formulation using FSDT

The displacement components for a node located in Mindlin plate, expressed as

$$u_\alpha(x,y,z) = -z\theta_\alpha(x,y) \quad , \quad u_3(x,y,z) = w(x,y) \quad , \alpha = 1,2 \tag{6}$$

Where u_1, u_2, and u_3 are the displacement components of a point located in middle plane in the x, y, and z directions, and θ_1, θ_2 are rotations of the transverse normal that perpendicular to the undeformed mid-plane in in the x – z and y – z surface, respectively. The relations between θ_1, θ_2 with transverse shear strains parameters γ_1, γ_2 are expressed as [11, 12]:

$$\theta_\alpha = (u_3)_{,\alpha} - \gamma_\alpha \quad , \alpha = 1,2 \tag{7}$$

According to the assumptions of Mindlin governing equations, normal and shear strain vectors are expressed based on displacement field components [12].

$$\varepsilon_b = \begin{bmatrix} \varepsilon_{11} \\ \varepsilon_{22} \\ \varepsilon_{12} \end{bmatrix} = z \begin{bmatrix} \theta_{1,1} \\ \theta_{2,2} \\ \theta_{1,2} + \theta_{2,1} \end{bmatrix} \tag{8}$$

$$\varepsilon_s = \begin{bmatrix} \gamma_1 \\ \gamma_2 \end{bmatrix} = \begin{bmatrix} w_{,1} + \theta_1 \\ w_{,2} + \theta_2 \end{bmatrix} \tag{9}$$

The terms of ε_s, ε_b are shear and bending strain respectively. Based on Hook's law, the relationships between stress and strain components are expressed as follows:

$$\begin{bmatrix} \sigma_x \\ \sigma_y \\ \sigma_{xy} \end{bmatrix} = z\, D_b \begin{bmatrix} \varepsilon_{xx} \\ \varepsilon_{yy} \\ \varepsilon_{xy} \end{bmatrix} \quad , \quad \begin{bmatrix} \tau_x \\ \tau_y \end{bmatrix} = D_s \begin{bmatrix} \gamma_x \\ \gamma_y \end{bmatrix} \tag{10}$$

3.2. Governing equations

Based on the first order theory (FSDT) and in absence of external load, the variation of total potential energy of whole plate in effect of normal and shear tension of buckling stress is obtained as follows [13]

$$\Pi=\frac{1}{2}\iint\delta\varepsilon_b^T \mathrm{D}_b\varepsilon_b \mathrm{d}x\mathrm{d}y+\frac{1}{2}\iint\delta\varepsilon_s^T \mathrm{D}_s\varepsilon_s \mathrm{d}x\mathrm{d}y+\frac{h}{2}\iint\begin{bmatrix}w_{,x} & w_{,y}\end{bmatrix}\hat{\sigma}_0\begin{Bmatrix}w_{,x}\\ w_{,y}\end{Bmatrix}\mathrm{d}x\mathrm{d}y$$

$$+\frac{h^3}{24}\iint\begin{bmatrix}\theta_{x,x} & \theta_{x,y}\end{bmatrix}\hat{\sigma}_0\begin{Bmatrix}\theta_{x,x}\\ \theta_{x,y}\end{Bmatrix}\mathrm{d}x\mathrm{d}y+\frac{h^3}{24}\iint\begin{bmatrix}\theta_{y,x} & \theta_{y,y}\end{bmatrix}\hat{\sigma}_0\begin{Bmatrix}\theta_{y,x}\\ \theta_{y,y}\end{Bmatrix}\mathrm{d}x\mathrm{d}y+\frac{1}{2}\iint\delta u^T M_m\ddot{u}\mathrm{d}x\mathrm{d}y=0 \tag{11}$$

Using Principle of virtual work, the elastic coefficients matrix for plate for first and second terms of Eq. 11 are expressed as:

$$B=\frac{E}{1-\nu^2}\begin{bmatrix}1 & \nu & 0\\ \nu & 1 & 0\\ 0 & 0 & \frac{1-\nu}{2}\end{bmatrix} \quad , \quad S=\frac{E}{1-\nu^2}\begin{bmatrix}\frac{1-\nu}{2} & 0\\ 0 & \frac{1-\nu}{2}\end{bmatrix} \tag{12}$$

Now by Integration on the plate thickness, the elastic coefficients of Eq. 11 are obtained as:

$$D_{bij}=\int_{-h/2}^{h/2} B_{ij} z^2\, dz \;\; i,j=1,2,3 \quad , \quad D_{skl}=\int_{-h/2}^{h/2} S_{kl}\, dz \quad k,l=1,2 \tag{13}$$

$$D_{b11}=\frac{E_b h^3}{12(1-\nu^2)} \tag{14}$$

$$D_{s11}=\frac{hE}{2(1+\nu)} \tag{15}$$

$$D_{b12}=D_{b21}=\nu D_{b11}, \quad D_{b13}=D_{b31}=0, \quad D_{b33}=\frac{1-\nu}{2} D_{b11} \tag{16}$$

$$D_{s22}=D_{s11}, \quad D_{s12}=D_{s21}=0 \tag{17}$$

Buckling coefficient of tensions matrix is shown as:

$$\hat{\boldsymbol{\sigma}}_0=\begin{bmatrix}\sigma_x^0 & \tau_{xy}^0\\ \tau_{xy}^0 & \sigma_y^0\end{bmatrix} \tag{18}$$

Each value of mass matrix obtains by integration from density matrix of Eq. 11 defined as:

$$M_{m11}=\int_{-h/2}^{h/2}\rho\, dz \;\; M_{m22}=M_{m33}=\int_{-h/2}^{h/2}\frac{\rho z^2}{12} dz \tag{19}$$

$$M_{m\,12} = M_{m\,13} = M_{m\,21} = M_{m\,23} = 0$$
$$M_{m\,31} = M_{m\,32} = 0 \tag{20}$$

3.3. Discrete form of Governing equations

Based on Mindlin/ Riesener theory, the transverse deflection at mid-plane and normal rotations in x and y directions are approximated by NEM shape functions as:

$$u^{a}{}_{(x)} \cong \sum_{i=1}^{np} \varphi_i^a(x)\, u_i \tag{21}$$

u_i is the nodal unknown variable of node i, φ_i is shape function of node i and (np) shows the number of nodes located in vicinity of ith node. Now by substituting Eq. (21) in Eq. (11), general equation would be separated base on shape functions and their derivatives.

$$\mathrm{u} = \sum_{i}^{np} \varphi_i \mathbf{d}_i, \quad \varepsilon_b = \sum_{i=1}^{np} B_{bi}\mathbf{d}_i, \quad \varepsilon_s = \sum_{i=1}^{np} B_{si}\mathbf{d}_i \tag{22}$$

$$\begin{Bmatrix} w_{,x} \\ w_{,y} \end{Bmatrix} = \sum_{i=1}^{np} \mathbf{G}_{bi}\mathbf{d}_i \quad , \quad \begin{Bmatrix} \theta_{x,x} \\ \theta_{x,y} \end{Bmatrix} = \sum_{i=1}^{np} \mathbf{G}_{s1i}\mathbf{d}_i \tag{23}$$

$$\begin{Bmatrix} \theta_{y,x} \\ \theta_{y,y} \end{Bmatrix} = \sum_{i=1}^{np} \mathbf{G}_{s2i}\mathbf{d}_i \tag{24}$$

$$u_i = \sum_{i=1}^{np} N_i\, d_i \tag{25}$$

Unknown vectors in each node, including the thickness and rotations along x and y axes are

$$\mathbf{u} = \begin{bmatrix} w & \theta_x & \theta_y \end{bmatrix}^T, \quad \mathbf{d}_i = \begin{bmatrix} w & \theta_{xi} & \theta_{yi} \end{bmatrix}^T \tag{26}$$

In these equations, stiffness matrix components form two bending and shear parts which are defined as:

$$\mathrm{B}_{bi} = \begin{bmatrix} 0 & \varphi_{i,x}^a & 0 \\ 0 & 0 & \varphi_{i,y}^a \\ 0 & \varphi_{i,y}^a & \varphi_{i,x}^a \end{bmatrix} \tag{27}$$

$$\mathrm{B}_{si}=\begin{bmatrix}\varphi_{i,x}^{a} & \varphi_{i}^{a} & 0\\ \varphi_{i,y}^{a} & 0 & \varphi_{i}^{a}\end{bmatrix} \tag{28}$$

Geometric and mass matrices of plate are shown as;

$$G_{bi}=\begin{bmatrix}\varphi_{i,x}^{a} & 0 & 0\\ \varphi_{i,y}^{a} & 0 & 0\end{bmatrix}\ G_{s1i}=\begin{bmatrix}0 & \varphi_{i,x}^{a} & 0\\ 0 & \varphi_{i,y}^{a} & 0\end{bmatrix}\ G_{s2i}=\begin{bmatrix}0 & 0 & \varphi_{i,x}^{a}\\ 0 & 0 & \varphi_{i,y}^{a}\end{bmatrix} \tag{29}$$

$$\mathrm{N}_{i}=\begin{bmatrix}\varphi_{i}^{a} & 0 & 0\\ 0 & \varphi_{i}^{a} & 0\\ 0 & 0 & \varphi_{i}^{a}\end{bmatrix} \tag{30}$$

Using the principle of minimum potential energy, based on shape functions and derivatives of shape functions, plate geometric, stiffness and mass stiffness matrices are expressed as:

$$\mathbf{K}_{\mathbf{G}}=h\int_{\Omega}\mathbf{G}_{b}^{T}\hat{\boldsymbol{\sigma}}_{0}\mathbf{G}_{b}d\Omega+\frac{h^{3}}{12}\int_{\Omega}\mathbf{G}_{s1}^{T}\hat{\boldsymbol{\sigma}}_{0}\mathbf{G}_{s1}d\Omega+\frac{h^{3}}{12}\int_{\Omega}\mathbf{G}_{s2}^{T}\hat{\boldsymbol{\sigma}}_{0}\mathbf{G}_{s2}d\Omega \tag{31}$$

$$\mathbf{K}=\int_{\Omega}\mathbf{B}_{b}^{T}\mathbf{D}_{b}\mathbf{B}_{b}d\Omega+\int_{\Omega}\mathbf{B}_{s}^{T}\mathbf{D}_{s}\mathbf{B}_{s}d\Omega \tag{32}$$

$$\mathbf{M}=\int_{\Omega}\mathrm{N}^{T}\,\mathrm{M}_{m}\mathrm{N}\,d\Omega \tag{33}$$

Stiffness matrices and geometry matrices of whole plate can be obtained by numerical integration of the governing equations. The critical buckling loads of plate are obtained by applying the boundary conditions on matrices.

$$(\mathbf{K}-\lambda\mathbf{K}_{G})\mathbf{d}=0 \tag{34}$$

Hence, Free vibration analyses such as natural frequencies and mode shapes of moderately thick plate base on NEM formulation are obtained as follows:

$$(\mathbf{K}-\omega^{2}\mathbf{M})\mathbf{d}=0 \tag{35}$$

4. The function of Program

Firstly, physical parameters of plate such as elastic modulus, Poisson's ratio, plate dimension and a cloud of nodes scattered on the plate domain should be determined. Then, Voronoi cells and Delaunay triangles are calculated. After that, numbers of Gaussian points in each Delaunay triangle are determined. Moreover, second Voronoi cell, shape function and first derivative of shape function are calculated for each gauss point. Now by substitution these relations in Eqs. (31, 32, 33) and using numerical integration method, stiffness, geometric and mass matrices

are determined. Finally, by imposing boundary conditions on problem domains, critical buckling load and vibration modes of plate are obtained by using Eqs.34and35.

5. Numerical examples

5.1. Natural frequency of plate

The properties of the steel plate considered here are as follows: elastic coefficient $E = 200Gpa$, density, $\rho = 7800 \, {Kg}/{m^3}$, Poisson's ratio $v = 0.3$ and the flexural rigidity $D = \frac{Eh^3}{12(1-v^2)}$, h/a the ratio of thickness to length . h/a has been assumed as $1/25$. Numerical results are good agreement with analytical solution obtained from eq. 36 for the same conditions of plate shown in table (1) .[14]

$$\hat{\omega}_{mn} = (m^2 + n^2)\frac{\pi^2}{a^2}\sqrt{\frac{D}{\rho h}} \text{ , } m,n = 1,2,3,....,\infty \tag{36}$$

Table 1. Natural frequencies of thin plate with a simply support conditions

Natural frequencies					Vibrations modes
NEM- number of node				analytical result	
49	121	441	961		
2300	1670	1305	1253	1210	(1,1)
5805	4388	3385	3159	3024	(2,1),(1,2)
10289	7355	5391	5140	4839	(2,2)

The natural frequencies of moderate thick plate converge to exact solution (eq.36) faster than thin plate results. Mindlin/ Riesener Theory consider shear strain terms so have better result for thick plate frequencies.

$$\omega_{mn}^2 = \left\{ \begin{array}{l} \left[1 + \frac{1}{12}\hat{\omega}_{mn}h^2\sqrt{\frac{\rho h}{D}}(1 + \frac{2}{(1-v)})\right] - \\ -\sqrt{\left[1 + \frac{1}{12}\hat{\omega}_{mn}h^2\sqrt{\frac{\rho h}{D}}(1 + \frac{2}{(1-v)})\right]^2 - \frac{\rho h^2}{3G\bar{\omega}_{mn}^2}} \end{array} \right\} \tag{36}$$

Table 2. Natural frequencies of thick plate with a simply support conditions

Natural frequencies								Vibrations modes
NEM- number of node						Analytical results		
121		441		961				
$\frac{h}{a}=\frac{1}{10}$	$\frac{h}{a}=\frac{1}{20}$	$\frac{h}{a}=\frac{1}{10}$	$\frac{h}{a}=\frac{1}{20}$	$\frac{h}{a}=\frac{1}{10}$	$\frac{h}{a}=\frac{1}{20}$	$\frac{h}{a}=\frac{1}{10}$	$\frac{h}{a}=\frac{1}{20}$	
3148	5479	2979	5380	2947	5362	2906	5259	(1,1)
7823	12248	7184	11830	7065	11753	6869	11340	(2,1),(1,2)
1206	18305	11150	17705	10985	17590	10519	16250	(2,2)

Mode shapes of plate are obtained after finding the displacement of each node shown as:

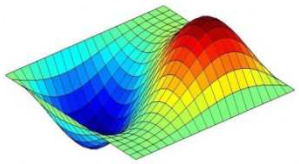

Figure 5. Second mode shape

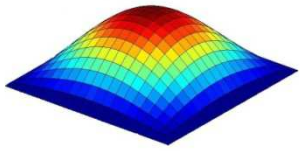

Figure 4. First mode shape

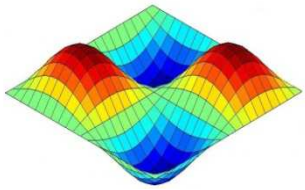

Figure 7. Fourth mode shape

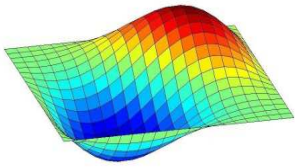

Figure 6. Third mode shape

Natural frequencies of parallelogram plate with two clamped edges are expressed in table (3). The angle between y axis and clamped edge is 45 degree and other edges of plate in x direction are free.

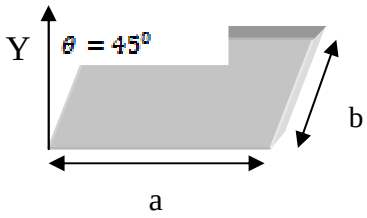

Figure 8. Schematic of parallelogram plate

Table 3. Natural frequencies of thick plate with CFCF boundary conditions

a/b	h/b	Vibrations modes	Number of nodes				Analytical results[14]
			64	121	256	441	
1	0.1	First mode	5529	5233	5049	5020	4905
		Second mode	5928	5504	5237	5191	5030
		Third mode	9590	8867	8467	8359	8093
		Fourth mode	17837	12020	11508	11306	10877
1	0.2	Vibrations modes					Analytical results[14]
		First mode	8302	8135	8024	8013	7765
		Second mode	8657	8368	8223	8205	7943
		Third mode	13710	13255	13005	12933	12523
		Fourth mode	17837	16920	16615	16542	15915

Mode shapes of plate CFCF boundary conditions are obtained after finding the displacement of each node shown as:

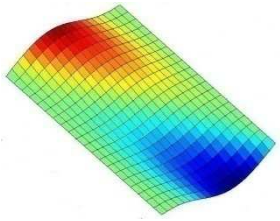

Figure 10. Second mode shape

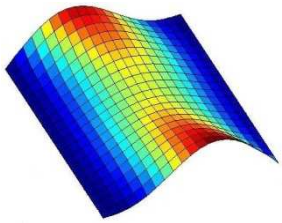

Figure 9. First mode shape

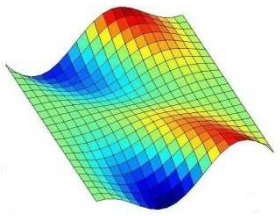

Figure 12. Fourth mode shape

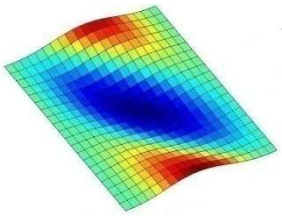

Figure 11. Third mode shape

Additionally Natural frequencies of parallelogram plate with one clamped edge in x direction (a) are expressed in table (4). Other edges are free and the angle between y axis and free edge is 30 degree.

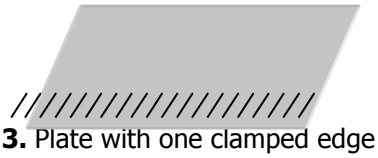

Figure 13. Plate with one clamped edge in x direction

Table 4. Natural frequencies of thick plate with CFFF boundary conditions

a/b	h/b	Vibrations modes	Number of nodes				Analytical results[14]
			64	121	256	441	
1	0.1	First mode	617	612	602	594	591
		Second mode	1426	1408	1391	1368	1359
		Third mode	3741	3696	3649	3586	3559
		Fourth mode	3938	3879	3829	3757	3719
		Fifth mode	5998	5931	5850	5738	5674
1	0.2	Vibrations modes					Analytical results[14]
		First mode	1168	1154	1151	1146	1139
		Second mode	2536	2506	2498	2491	2468
		Third mode	6165	6098	6087	6049	5979
		Fourth mode	6803	6714	6704	6636	6540
		Fifth mode	9786	9647	9598	9517	9368

Six first Mode shapes of plate CFFF boundary conditions are determinded after finding the displacement of each node shown as:

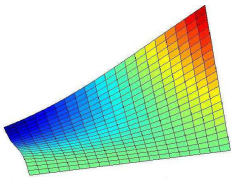

Figure 15. Second mode shape

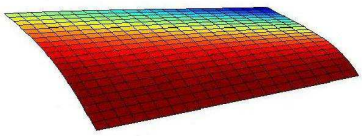

Figure 14. First mode shape

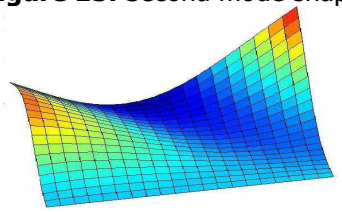

Figure 17. Fourth mode shape

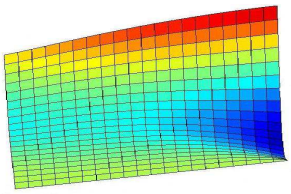

Figure 16. Third mode shape

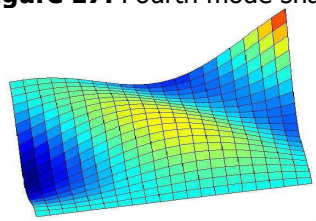

Figure 19. sixth mode shape

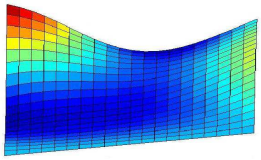

Figure 18. Fifth mode shape

5.2. Buckling Analysis of Plates

Critical buckling load of rectangular plate is determined by NE method. The ratio of length to thickness is 0.1 and boundary conditions are assumed clamped for all edges of plate. Based on Torsional stiffness coefficient D (Eq.37) Critical load is obtained Dimensionless. .[Wang et al [15]]

$$D = Eh^3 / 12(1-\nu^2), \qquad \lambda_{cr} = \mathrm{P}\, a^2 / \pi^2 \mathrm{D} \tag{37}$$

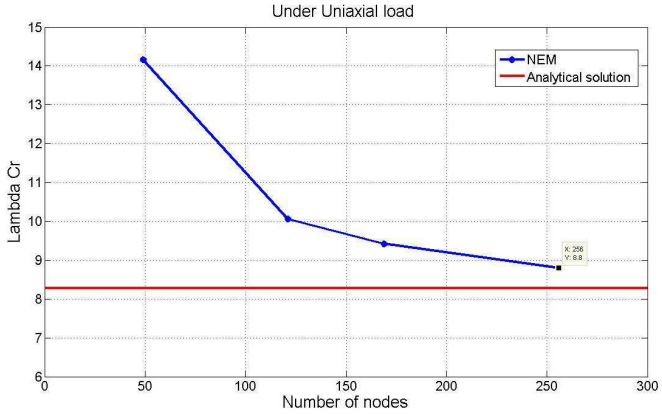

Figure 20. Non-dimensional buckling parameter for fully clamped plate under uniaxial load

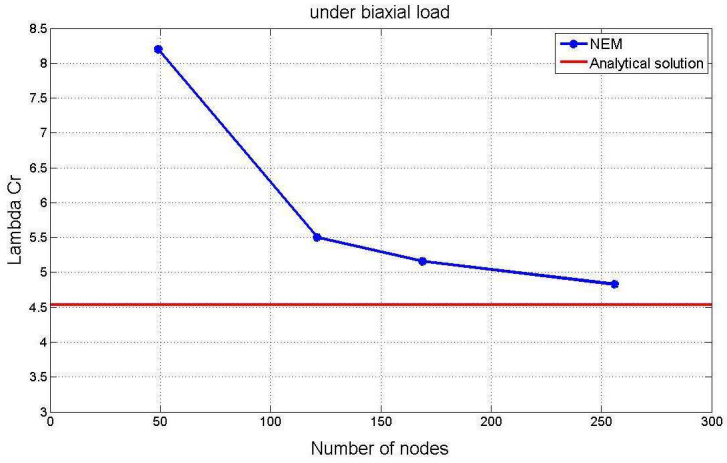

Figure 21. Non-dimensional buckling parameter for fully clamped plate under biaxial load

6. Conclusions

In this article the natural element method was used to study free vibration and buckling behavior of thin and thick plates. To this end, Mindlin-Reisener theory was utilized. The equations were generalized by using FSDT method. Comparing the results of the natural element method with those obtained by analytical method and other MFM, it was shown that present method can predict buckling loads and free vibration modes of plates accurately. It was observed that increas-

ing the number of nodes results in raising the accuracy of results. Since the governing relations are extracted from Mindlin theory, increasing the thickness of plates leads to faster convergence of numerical answers to analytical ones. Besides, dependency on the numbers of nodes decreased. NEM method has the ability to analyze plates with complex geometries and various ranges of boundary conditions. Another merit of this method in comparison with FEM is simplification of the analyses by the user.

References

[1] Cai Y., Zhu H., *A local search algorithm for natural neighbours in the natural element method*, International Journal of Solids and Structures v.42 ,2005, pp. 6059–6070.

[2] Braun J., Sambridge M., *A numerical method for solving partial differential equations on highly irregular evolving grids*. Nature, v.376, 1995, pp. 655- 660.

[3] Belytschko T., Lu Y., Gu L., *Element-free Galerkin methods* , International Journal for Numerical Methods in Engineering, v.37, 1994, pp. 229-256.

[4] Cho J.R., Lee H.W., *Polygon-Wise constant curvature natural element approximation of Kirchhoff plate model*, International Journal of Solid and structures, v.44, 2007,pp.4860-4871.

[5] Zhang Y., Yi H.L., Tan H. P.,*Natural element method analysis for coupled radiative and conductive heat transfer in semitransparent medium with irregular geometries*, International Journal of Thermal Sciences. v76, 2014, pp.30-42.

[6] Chen S.S., Li Q.H., Liu Y.H., Xue Z.Q., *A meshless local natural neighbour interpolation method for analysis of two-dimensional piezoelectric structures,* Engineering Analysis with Boundary Elements Vol.37, 2013,pp.273–279.

[7] Reddy J.N., Phan N.D., *Stability and vibration of isotropic, orthotropic and laminated plates according to a higher-order shear deformation theory,* Journal of Sound and Vibration, vol. 98 (2),1985, pp. 157–170.

[8] Zenkour A.M., Buckling and free vibration of elastic plates using simple and mixed shear deformation theories, ACTA Mechanica, vol.145, 2001 ,pp.183–197.

[9] Liew K.M., Xiang Y., Kitipornchai S., *Analytical buckling solutions for mindlin plates involving free edges*, International Journal of Mechanical Sciences, vol. 38 (10), 1996, pp.1127–1138.

[10] Sukumar N., Moran B., Belytshko T., *The natural element method in solid mechanics*, international Journal for Numerical Methods in Engineering, v.43(5) , 1998, pp. 839-887.

[11] Reddy J.N., *Theory and Analysis of Elastic Plates,* Taylor & Francis , MI.1999.
[12] Hughes T.J.R., *The finite Element Method: Linear Static and Dynamic Finite Element Analysis*, Prentice Hall, Englewood Cliffs, 1987.
[13] Shmuel L.W., Taylor R.L., *Mixed formulations for plate bending elements*, Computer Methods in Applied Mechanics and Engineering, vol. 94, 1992, pp.391-427.
[14] Liew, K.M., Wang. C.M., Xiang. Y., Kitpornchai. S., *Vibration of Mindlin Plate*, Elsevier Science Ltd, 1998.
[15] Wang CM, Liew KM, Xiang Y., Kitipornchai S., *Buckling of rectangular Mindlin plates with internal supports*, nt J Solids Struct; vol.30, 1993, pp.1–17.

Addresses:

- PhD candidate. Mohammad Etemadi, "Langaroud" University, Department of Mechanical Engineering, Islamic Azad University, Langaroud branch, Guilan, Iran, etemadi@iaul.ac.ir
- PhD candidate. Fakhri Etemadi, Aerospace engineering of Amirkabir University of Technology Tehran, Iran
- Eng. Tayeb Pourreza, "Langaroud" University, Department of Mechanical Engineering, Islamic Azad University, Langaroud branch, Guilan, Iran, pourreza@iaul.ac.ir